Photon distribution function for propagation of two-photon pulses in waveguide-qubit systems

Oleksandr O. Chumak* and Evgeniy V. Stolyarov
Institute of Physics, National Academy of Sciences of Ukraine, Prospekt Nauki 46, 03028 Kyiv, Ukraine
(Received 10 October 2014; published 22 December 2014)

Propagation of a two-photon pulse in a waveguide coupled to a two-level system (TLS) is studied. The pulse is formed by two spatially separated identical wave packets. A set of equations governing the dynamics of the photon distribution in the configuration-momentum space is derived and solved. It is shown that the distribution function can be negative, which manifests its quasiprobability nature. A spectrum of the reflected light is found to be narrower than that of the transmitted light that features a pronounced filtering effect. Average numbers of the transmitted and reflected photons and their variances are shown to be dependent not only on the pulse widths and the light-TLS interaction but also on the pulse separation that can serve as an effective controlling parameter. Our approach is generalized for the case of an n-photon Fock state.

DOI: 10.1103/PhysRevA.90.063832 PACS number(s): 42.50.Ct, 42.50.Ar, 42.50.Pq

I. INTRODUCTION

The problem of interaction of few-photon pulses with two-level systems (TLSs) attracts an increasing interest. First, this is due to the development of quantum information processing (QIP) devices. The TLSs are the simplest implementations of the stationary quantum bits (qubits). In practice, various multilevel systems are used: trapped ions [1,2] or neutral atoms [3], superconducting Josephson junctions [4], semiconductor quantum dots [5], etc. Nevertheless, in many cases those multilevel systems can be modeled as TLSs. This simplification is quite reasonable if the frequency of the incident radiation is close to the transition frequency between the corresponding pair of levels.

Recent experiments show that photons can act as transmitters of quantum states between distant stationary qubits [6,7]. Moreover, stationary qubits are able to controllably generate correlations between photons. The qubits, connected by optical or microwave waveguides, form scalable chip-based circuits [8]. These circuits are considered now as a potential hardware basis for the QIP systems. Properties of photons propagating in waveguide-qubit systems have attracted increasing interest.

Theoretical description of propagation of few-photon pulses in waveguides coupled to a TLS can be found in numerous publications [9–18]. For example, a collision of two wave packets at a TLS was studied [9]. A striking difference in the interaction of the Fock-state and coherent-state wave packets of the same photon number was illustrated. It was shown that photon-TLS coupling induces correlation between photons that can be interpreted as their interaction. This controllable photon-photon interaction may be used for generation of spatiotemporal entanglement and four-wave mixing effects [10,11].

Evolution of the photon-TLS was studied in the Heisenberg picture in Ref. [9]. In contrast, the authors of Refs. [10–16] preferred the Schrödinger picture. The theoretical analysis is simplified if the incoming and outgoing radiation fields are away from the TLS and, accordingly, are outside of the interaction range. In those regions the evolution of fields is as if there is no interaction with the TLS. In this situation the initial and the final states of the radiation are connected by the S matrix whose elements can be extracted from the eigenstates of the full interacting Hamiltonian. Provided that the S matrix is known, the outgoing field can be expressed via the entering field. A rigorous program to construct the complete scattering matrix, which is applicable for two or more photons, was developed in Refs. [13–16]. Using that technique the physical quantities such as transmission or reflection coefficients can be obtained analytically. The above approach was extended in Ref. [16] for coherent-state wave packets with arbitrary photon numbers.

Further studies [17,18] were based on the input-output formalism of quantum optics [19]. One- and two-photon scattering with a TLS was analyzed. The relationship between the input-output operators, which are inherent for the Heisenberg picture of the evolution equations, and the photon scattering matrix was derived. It was shown that these approaches are equivalent. At the same time the authors of Ref. [17] inferred that the input-output approach was more elementary than the techniques developed earlier in Refs. [12–14].

The Heisenberg picture is suitable for using the phase-space distribution function [20], which provides a comprehensive description of the system. Within this approach the evolution of wave packets in the coordinate space as well as in the momentum space can be analyzed in detail [21]. The operator of the phase-space distribution function, $\hat{f}(x,p,t)$, represents the photon density in the coordinate-momentum (x,p) phase space. It was shown in Ref. [21] that the average value of the phase-space distribution function, $\langle\hat{f}(x,p,t)\rangle$, may be negative at some domains of phase space, which indicates that $\langle\hat{f}(x,p,t)\rangle$ corresponds to a quasiprobability rather than the probability of the photon density in the phase space.

In this work, we extend our previous studies [21] to the case of few-photon Fock states of the ingoing field. We consider dynamics in the phase space and statistical properties of two-photon pulses whose initial state is represented by a sequence of two single-photon wave packets. The initial distance between them is a free parameter, which controls the correlation of outgoing photons. Then we outline a general scheme to study systems with an arbitrary number of photons.

The paper is organized as follows. The model Hamiltonian and the initial state are drawn in Sec. II. In Sec. III the set

*chumak@iop.kiev.ua

of equations describing dynamics of the system is derived and solved. Dynamics of the qubit for different parameters of the system is analyzed. Evolution of two-photon pulses in the phase-space is studied. In Sec. IV the statistical properties of the outgoing photons are investigated. The obtained results are summarized in Sec. V. Derivation of useful operator relations used throughout the paper is delegated to Appendix A. In Appendix B we demonstrate a generalization of the method for the case of an n-photon Fock-state input.

II. MODEL

A. Hamiltonian of the model

The system we study consists of a TLS (qubit) coupled to photons propagating in both directions in a one-dimensional waveguide. Figure 1 displays the scheme of the model system. Ground and excited states of the TLS are denoted as $|g\rangle$ and $|e\rangle$, respectively. The system is modeled by the Hamiltonian

$$\hat{\mathcal{H}} = \hat{\mathcal{H}}_0 + \hat{\mathcal{H}}_{\rm int}. \tag{1}$$

Here $\hat{\mathcal{H}}_0$ describes the free evolution of a TLS and the field in the waveguide. Assuming that the waveguide modes form a one-dimensional continuum [22], it is given by

$$\hat{\mathcal{H}}_0 = \omega_a\, \sigma_+ \sigma_- + \int dp\, \left(\omega_p^l\, l_p^\dagger\, l_p + \omega_p^r\, r_p^\dagger\, r_p\right), \tag{2}$$

where ω_a is the transition frequency, $\sigma_+ = |e\rangle\langle g|$ and $\sigma_- = |g\rangle\langle e|$ are raising and lowering operators obeying the Pauli matrices algebra, $l_p^\dagger(l_p)$ and $r_p^\dagger(r_p)$ are respectively bosonic creation (annihilation) operators of the photons propagating in the waveguide from the left to the right side and vice versa. In what follows we use terms "l − mode" ("l − photon") and "r-mode" ("r-photon") to denote the left-to-right and right-to-left propagating modes (photons), respectively. Photon frequencies, $\omega_p^{l,r}$, linearized with respect to momenta p (see Ref. [23]) are defined as $\omega_p^{l,r} = \omega_0 \pm v_g\, p$, where ω_0 is the central frequency and $v_g > 0$ is the group velocity. This Hamiltonian is referred to as the two-mode model [17]. Throughout the paper we set the Planck's constant $\hbar$ to 1 and, thus, measure momentum and energy in wave number and frequency units, correspondingly.

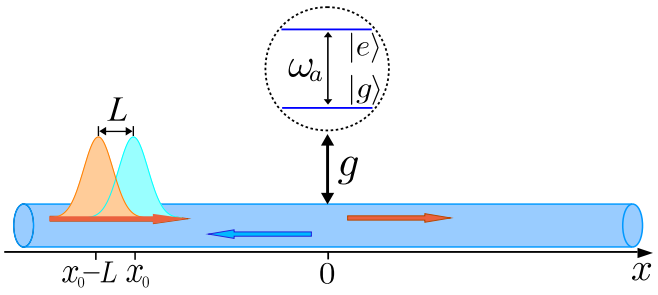

FIG. 1. (Color online) Scheme of the system under consideration. A qubit modeled by a TLS is positioned at $x = 0$ and coupled equally to waveguide modes propagating from the left to the right and vice versa. The ingoing two-photon state is represented by two single-photon pulses, which can be separated by distance L. The initial positions of the pulses are x_0 and $x_0 - L$.

The other constituent of the full Hamiltonian (1) describes interaction of the radiation field with the TLS. In the rotating-wave approximation it is given by

$$\hat{\mathcal{H}}_{\rm int} = g \int dp (l_p^\dagger + r_p^\dagger)\sigma_- + \text{H.c.}, \tag{3}$$

where g is the frequency-independent waveguide-qubit coupling strength.

The total number of excitations in the system is defined by the operator

$$\hat{N}_{\rm ex} = \int dp [l_p^\dagger\, l_p + r_p^\dagger\, r_p] + \sigma_+\, \sigma_-, \tag{4}$$

which, similar to (2), does not contain the interaction terms. Using the definition (4) the Hamiltonian (2) is rewritten as

$$\hat{\mathcal{H}}_0 = \omega_0\, \hat{N}_{\rm ex} + \Delta\, \sigma_+\, \sigma_- + v_g \int dp\; p[l_p^\dagger\, l_p - r_p^\dagger\, r_p],$$

where $\Delta = \omega_a - \omega_0$ is the detuning between the TLS transition frequency and the central frequency of the waveguide modes.

The operator $\hat{N}_{\rm ex}$ commutes with the Hamiltonian, $[\hat{N}_{\rm ex}, \hat{\mathcal{H}}] \equiv 0$. Hence, it is the integral of motion. Thus, the system can be equivalently described by the modified Hamiltonian

$$\hat{\mathcal{H}}' = \hat{\mathcal{H}} - \omega_0\, \hat{N}_{\rm ex} = \hat{\mathcal{H}}_0' + \hat{\mathcal{H}}_{\rm int}, \tag{5}$$

where

$$\hat{\mathcal{H}}_0' = v_g \int dp\; p[l_p^\dagger\, l_p - r_p^\dagger\, r_p] + \Delta\, \sigma_+\, \sigma_-.$$

B. Initial state of the system

We consider the dynamics of light propagating from the left to the right as shown in Fig. 1. It is assumed that initially (at $t = t_0$) the qubit is in the ground state, $|g\rangle$, and the propagating light is represented by two single-photon pulses $|1_\alpha\rangle$ and $|1_\beta\rangle$. They are superpositions of single-photon states $l_p^\dagger\,|0\rangle$ weighted by amplitudes α_p and β_p:

$$|1_\alpha\rangle = \int dp\, \alpha_p\, l_p^\dagger(t_0)\,|0\rangle \equiv a_\alpha^\dagger|0\rangle, \tag{6a}$$

$$|1_\beta\rangle = \int dp\, \beta_p\, l_p^\dagger(t_0)\,|0\rangle \equiv a_\beta^\dagger|0\rangle, \tag{6b}$$

where $|0\rangle$ is the vacuum state of the system and the factors α_p and β_p ensure the normalization conditions for states (6a) and (6b)

$$\int dp|\alpha_p|^2 = \int dp|\beta_p|^2 = 1.$$

It can be verified that $|1_{\alpha,\beta}\rangle$ are the eigenstates of the operator of the total photon number, $\hat{N}_l = \int dp\, l_p^\dagger\, l_p$, with the eigenvalues equal to unity

$$\hat{N}_l|1_{\alpha,\beta}\rangle = 1 \cdot |1_{\alpha,\beta}\rangle,$$

which indicates that $|1_{\alpha,\beta}\rangle$ are the single-photon Fock states. In what follows we set

$$\beta_p = \alpha_p\, e^{i\,p\,L}. \tag{7}$$

Then the configuration-space densities of photons in the initial states $|1_{\alpha,\beta}\rangle$ are related as

$$\langle 1_\beta|\hat{\rho}_l(x,t_0)|1_\beta\rangle = \langle 1_\alpha|\hat{\rho}_l(x+L,t_0)|1_\alpha\rangle, \tag{8}$$

where the operator of density of the l photons is given by [21]

$$\hat{\rho}_l(x,t) = \frac{1}{2\pi}\int dp\, dk\, e^{-i\,k\,x}\, l^\dagger_{p+k/2}(t)\, l_{p-k/2}(t). \tag{9}$$

All operators are defined in the Heisenberg representation with the Hamiltonian given by (5). It can be seen from (8) that the β and α pulses being separated by L have identical shapes. Acting by the raising operators $a^\dagger_\alpha$ and $a^\dagger_\beta$ on the vacuum state $|0\rangle$ we obtain a two-photon Fock state

$$|2_{\alpha\beta}\rangle = \nu\, a^\dagger_\beta\, a^\dagger_\alpha|0\rangle, \quad \nu = \frac{1}{\sqrt{1+|\chi|^2}}. \tag{10}$$

Parameter $\chi = \int dp\, \alpha^*_p\, \beta_p$ describes the overlap of the single-photon states (6a) and (6b). When $L = 0$ the constant ν is equal to $(2!)^{-1/2}$ and the definition of a two-photon state coincides with the usual definition of the n-photon Fock state given by $|n_\alpha\rangle = (a^\dagger_\alpha)^n|0\rangle/\sqrt{n!}$ [24].

It should be noted that there is another type of two-photon states named by quantum-correlated photon pairs. They are defined as (see, for example, Ref. [25])

$$|2_{\rm corr}\rangle = \frac{1}{\sqrt{2}}\int dp \int dp'\, \psi(p,p')\, l^\dagger_p\, l^\dagger_{p'}|0\rangle,$$

where $\psi(p,p') = \psi(p)\,\delta(p+p'-2p_0)$ and $2p_0$ is the total momentum of the photon pair. These states are referred to as the twin-beam states and can be obtained from spontaneous parametric down conversion. The δ function indicates energy anticorrelation of two photons.

We use here the definition (10). Let us assume that the ingoing pulses are given by Gaussian distributions. Then α_p is given by

$$\alpha_p = \frac{w^{1/2}}{\pi^{1/4}}\,\exp\left[-\frac{w^2\,p^2}{2} - i\,p\,x_0\right], \tag{11}$$

where w is the pulse width and $x_0 < 0$. Thus, the single-photon densities are

$$\begin{aligned}\langle 1_\alpha|\hat{\rho}_l(x,t_0)|1_\alpha\rangle &= \frac{1}{\pi^{1/2}\,w}\,e^{-(x-x_0)^2/w^2},\\ \langle 1_\beta|\hat{\rho}_l(x,t_0)|1_\beta\rangle &= \frac{1}{\pi^{1/2}\,w}\,e^{-(x+L-x_0)^2/w^2}.\end{aligned} \tag{12}$$

The photon density for the state $|2_{\alpha\beta}\rangle$ is given by

$$\begin{aligned}&\langle 2_{\alpha\beta}|\hat{\rho}_l(x,t_0)|2_{\alpha\beta}\rangle\\ &= \frac{\nu^2}{\pi^{1/2}\,w}\left[e^{-(x-x_0)^2/w^2} + e^{-(x+L-x_0)^2/w^2}\right.\\ &\quad \left. + 2e^{-L^2/2\,w^2}\,e^{-(x-x_0+L/2)^2/w^2}\right],\end{aligned} \tag{13}$$

where $\nu^{-2} = 1 + e^{-L^2/2\,w^2}$. For large L the coefficient ν^2 tends to unity and the last term in the square brackets, which describes the interference effect, vanishes. In this case the incoming field is represented by two independent single-photon pulses.

It can be seen from Eq. (13), illustrated by Fig. 2, that the densities at $x = x_0$ and $x = x_0 - L$ are slightly smaller than those given by Eqs. (12). On the contrary, the density at the intermediate position $x = x_0 - L/2$ increases. This variation of the photon density is caused by interference of the incoming fields. Also, this phenomenon can be interpreted as a photon-photon interaction caused by quantum correlations of the incoming pulses.

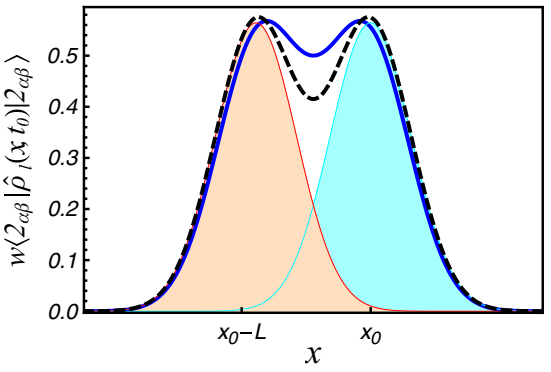

FIG. 2. (Color online) The initial photon distributions in the configuration space for $L = 2\,w$. Solid thin lines indicate the densities of photons in the states $|1_\alpha\rangle$ and $|1_\beta\rangle$. Dashed line is the sum of these densities. Solid thick line is the density in the two-photon Fock state $|2_{\alpha\beta}\rangle$. The areas under the dashed and solid lines are both equal to 2. Coordinate x is measured in units of w.

III. EQUATIONS OF MOTION AND EVOLUTION OF TWO-PHOTON FIELD

Followed from Hamiltonian (5) the Heisenberg equations of motion for photon variables $l_p(t)$ and $r_p(t)$ are as follows

$$(\partial_t + i\,v_g\,p)l_p = -i\,g\,\sigma_-, \tag{14a}$$

$$(\partial_t - i\,v_g\,p)r_p = -i\,g\,\sigma_-, \tag{14b}$$

with solutions

$$l_p(t) = \tilde{l}_p(t) - i\,g\int_{t_0}^{t} d\tau\, e^{-i\,v_g\,p\,(t-\tau)}\,\sigma_-(\tau), \tag{15a}$$

$$r_p(t) = \tilde{r}_p(t) - i\,g\int_{t_0}^{t} d\tau\, e^{i\,v_g\,p\,(t-\tau)}\,\sigma_-(\tau), \tag{15b}$$

where $t > t_0$. Tildes over the operators indicate their free evolution:

$$\tilde{l}_p(t) = l_p(t_0)\,e^{-i\,v_g\,p\,(t-t_0)}, \quad \tilde{r}_p(t) = r_p(t_0)\,e^{i\,v_g\,p\,(t-t_0)}. \tag{16}$$

Using Hamiltonian (5), Eqs. (15a) and (15b), the equations of motion for the qubit variables take the forms

$$(\partial_t + \Gamma)\sigma_+\sigma_- = i\,g\int dp(\tilde{l}^\dagger_p + \tilde{r}^\dagger_p)\sigma_- + \text{H.c.}, \tag{17}$$

$$(\partial_t + i\,\Delta + \Gamma/2)\sigma_- = i\,g(2\,\sigma_+\sigma_- - 1)\int dp(\tilde{l}_p + \tilde{r}_p), \tag{18}$$

where $\Gamma = 4\,\pi\,g^2/v_g$. Equation (17) indicates that parameter Γ is a decay rate of the qubit excitation. Effect of the ingoing field is accounted by the free-moving photon operators $\tilde{l}_p$ and $\tilde{r}_p$.

A. Qubit dynamics

Using Eqs. (17), (18) and the definition of the initial state (10) we obtain a full set of equations governing the TLS excitation dynamics:

$$(\partial_t + \Gamma)\,\langle\sigma_+\,\sigma_-\rangle = i\,g\left[A^*(t)\langle 1_\beta|\sigma_-|2\rangle + B^*(t)\langle 1_\alpha|\sigma_-|2\rangle\right] + \text{c.c.}, \tag{19a}$$

$$(\partial_t + i\,\Delta + \Gamma/2)\,\langle 1_\alpha|\sigma_-(t)|2\rangle = 2\,i\,g\,v\,\langle 1_\alpha|\sigma_+(t)|0\rangle[A(t)\,\langle 0|\sigma_-(t)|1_\beta\rangle + B(t)\,\langle 0|\sigma_-(t)|1_\alpha\rangle] - i\,g\,v\,[\chi\,A(t) + B(t)], \tag{19b}$$

where $A(t) = \int dp\, e^{-i\,v_g\,p\,t}\,\alpha_p$ and $B(t) = \int dp\, e^{-i\,v_g\,p\,t}\,\beta_p$. Here and in what follows the index $\alpha\beta$ in the denotation of the initial state $|2_{\alpha\beta}\rangle$ is omitted. The equation for $\langle 1_\beta|\sigma_-(t)|2\rangle$ can be obtained by mutual replacement of α and β as well as $A(t)$ and $B(t)$ in Eq. (19b). The explicit expression for $\langle 0|\sigma_-|1_{\alpha,\beta}\rangle$ follows from Eqs. (18) and (A2) and has the form

$$\langle 0|\sigma_-(t)|1_\alpha\rangle = -i\,g\int_0^t d\tau\, e^{-(i\,\Delta+\Gamma/2)(t-\tau)}\,A(\tau). \tag{20}$$

The expression for $\langle 0|\sigma_-(t)|1_\beta\rangle$ is obtained by replacing $A(t)$ with $B(t)$. For the sake of brevity, hereinafter we set $t_0 = 0$.

The evolution of the TLS excitation probability $\langle\sigma_+\,\sigma_-\rangle = (\langle\sigma_z\rangle + 1)/2$ for different values of Γ, Δ and L is displayed in Fig. 3. The calculations show that the strongest TLS excitation is observed when the bandwidth $\Omega = v_g/w$ of the ingoing pulse is close to the TLS decay rate Γ and $L = 0$. With decrease of Γ the TLS exhibits lower excitation and the lifetime of the excited state increases. The opposite scenario results in the inhibition of the TLS excitation and reduction of the excited state lifetime [see Fig. 3(a)]. Increase of the magnitude of detuning $|\Delta|$ leads to the reduction of the TLS excitation as can be seen in Fig. 3(b). In the limit of $\Delta \gg \Gamma$ the TLS excitation probability tends to zero. Figure 3(c) shows the qubit evolution for different values of the spatial separation between the ingoing pulses. For $L < \Gamma^{-1}$ the lifetime of the TLS excited state grows with increase of L whereas the maximum excitation probability drops down. Further increase of L results in the two-peak structure of the TLS excitation dependence on time. When $L \gg \Gamma^{-1}$ the TLS is excited as in the case of single-photon input. In this case the TLS has sufficient time to relax to the ground state forgetting about the first photon. Results presented in Fig. 3 show the possibility to control the state of the qubit by controlling the parameters of the ingoing pulses and qubit-photon interaction.

B. Phase-space evolution

The operator of the phase-space distribution function for the l photons is given by [21]

$$\hat{f}_l(x,p,t) = \frac{1}{2\pi}\int dk\, e^{-i\,k\,x}\,l^\dagger_{p+k/2}(t)\,l_{p-k/2}(t),$$

which is similar to those used for description of electrons and phonons in semiconductors [26].

In order to simplify further considerations we introduce photon operators $l(x,t)$ and $r(x,t)$ describing, respectively, annihilation of l photon and r photon at the coordinate x. They are defined as

$$l(x,t) = (2\pi)^{-1/2}\int dp\, e^{i\,p\,x}\,l_p(t),\qquad r(x,t) = (2\pi)^{-1/2}\int dp\, e^{i\,p\,x}\,r_p(t). \tag{21}$$

Substituting expressions (15a) and (15b) into Eq. (21) we obtain the following relations

$$l(x,t) = \tilde{l}(x,t) - i\,\sqrt{2\pi}\,\frac{g}{v_g}\,\sigma_-\left(t - \frac{x}{v_g}\right)\theta(x)\,\theta\left(t - \frac{x}{v_g}\right), \tag{22a}$$

$$r(x,t) = \tilde{r}(x,t) - i\,\sqrt{2\pi}\,\frac{g}{v_g}\,\sigma_-\left(t + \frac{x}{v_g}\right)\theta(-x)\,\theta\left(t + \frac{x}{v_g}\right), \tag{22b}$$

where $\theta(x)$ is the Heaviside step function. As previously, tildes indicate the free-propagating operators, which act on the initial state (10) as

$$\tilde{l}(x,t)|2\rangle = (2\pi)^{-1/2}\,v\left[A\left(t - \frac{x}{v_g}\right)|1_\beta\rangle + B\left(t - \frac{x}{v_g}\right)|1_\alpha\rangle\right], \tag{23a}$$

$$\tilde{r}(x,t)|2\rangle = 0. \tag{23b}$$

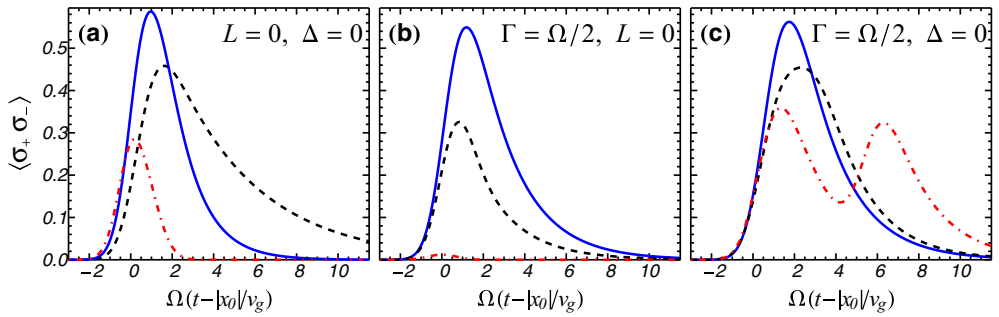

FIG. 3. (Color online) The TLS excitation dynamics: (a) $\Gamma = 3\Omega/4$ (blue solid line), $\Gamma = \Omega/4$ (black dashed line), $\Gamma = 5\Omega$ (red dash-dotted line); (b) $|\Delta| = \Omega/4$ (blue solid line), $|\Delta| = \Omega$ (black dashed line), $|\Delta| = 5\Omega$ (red dash-dotted line); (c) $L = w$ (blue solid line), $L = 2\,w$ (black dashed line), $L = 5\,w$ (red dash-dotted line).

Using (21) the operator of the phase-space distribution function for the l photons takes the form

$$\hat{f}_l(x,p,t) = \frac{1}{2\pi}\int d\xi\, e^{i\,p\,\xi}\, l^\dagger(x+\xi/2,t)\, l(x-\xi/2,t). \quad (24)$$

Substituting expression (22a) into (24) and taking into account (23a) we obtain the average value of the phase-space distribution for the l photons as

$$\langle \hat{f}_l(x,p,t)\rangle = \langle \tilde{f}_l(x,p,t)\rangle + \frac{\Gamma}{2\pi}\int_{-2x/v_g}^{2x/v_g} d\tau\, e^{-i\,v_g\,p\,\tau}\left\langle \sigma_+\left(t'+\frac{\tau}{2}\right)\sigma_-\left(t'-\frac{\tau}{2}\right)\right\rangle\Big|_{t'=t-x/v_g}$$
$$- i\,\frac{g\,\nu}{2\pi}\int_{2(x/v_g-t)}^{2x/v_g} d\tau\left\{e^{i\,v_g\,p\,\tau}\left[A^*\left(t'-\frac{\tau}{2}\right)\langle 1_\beta| + B^*\left(t'-\frac{\tau}{2}\right)\langle 1_\alpha|\right]\sigma_-\left(t'+\frac{\tau}{2}\right)|2\rangle - \text{c.c.}\right\}\Big|_{t'=t-x/v_g}. \quad (25)$$

The first term on the right-hand side of Eq. (25) describes free propagation of the initial pulse. The average value $\langle \tilde{f}_l(x,p,t)\rangle$ for distributions (7) and (11) is given by

$$\langle \tilde{f}_l(x,p,t)\rangle = \frac{\nu^2}{\pi}\, e^{-p^2 w^2}\left[e^{-X^2(t)/w^2} + e^{-[X(t)+L]^2/w^2} + 2\,\cos(pL)\, e^{-L^2/4w^2}\, e^{-[X(t)+L/2]^2/w^2}\right], \quad (26)$$

where $X(t) = x - x_0 - v_g\,t$. In this case $\langle \tilde{f}_l(x,p,t)\rangle$ depends only on two variables, i.e., $x - v_g\,t$ and p. Integration of $\langle \tilde{f}_l(x,p,t)\rangle$ over p gives the configuration-space distribution (13). Expression (26) shows that for the ingoing Gaussian pulse the initial phase-space distribution is positive at any point of phase space.

Figure 4 displays the initial phase-space distribution for $L = 3w$. This distribution exhibits a two-peak structure with maxima at x_0 and $x_0 - L$ as it follows from (26). The interference of the single-photon wave packets is described by the third term in the brackets in Eq. (26). For larger L the interference becomes less pronounced and the initial distribution tends to form two solitary peaks. For $L = 0$ the initial distribution has the only maximum at x_0.

The second and third terms on the right-hand side of Eq. (25) arise due to interaction of the ingoing pulse with the qubit. These terms are nonzero only for $x > 0$. The integration limits are imposed by the θ functions in Eqs. (22a) and (22b). The second term in (25) describes the l mode of the field reemitted by the TLS. The third term on the right-hand side of (25) is linear with respect to the waveguide-qubit coupling parameter g. This term describes interference of the ingoing field and the field reemitted by the TLS.

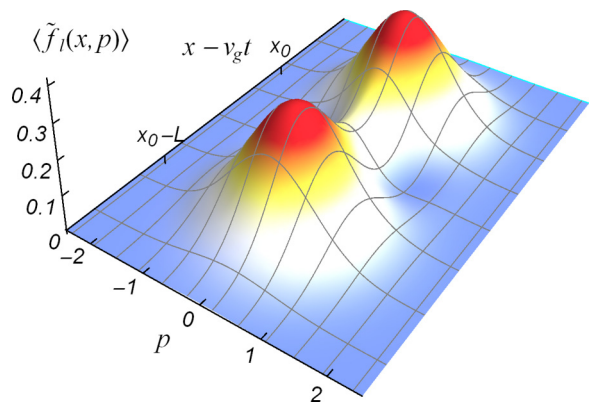

FIG. 4. (Color online) The initial photon phase-space distribution for $L = 3w$ exhibiting two-peak structure. Oscillations in the vicinity of $X(t) = -L/2$ are damped. Coordinate x and momentum p are measured in units of w and w^{-1}, respectively.

The operator of the phase-space distribution for the r photons, $\hat{f}_r(x,p,t)$, is defined by replacing l with r in (24). Taking into account Eqs. (22b) and (23b) we obtain $\langle \hat{f}_r(x,p,t)\rangle$ as

$$\langle \hat{f}_r(x,p,t)\rangle = \frac{\Gamma}{2\pi}\int_{2x/v_g}^{-2x/v_g} d\tau\, e^{i\,v_g\,p\,\tau}\left\langle \sigma_+\left(t'+\frac{\tau}{2}\right)\sigma_-\left(t'-\frac{\tau}{2}\right)\right\rangle\Big|_{t'=t+x/v_g}. \quad (27)$$

This distribution is nonzero for $x < 0$ and coincides with the second term on the right-hand side of Eq. (25), with v_g is replaced by $-v_g$, due to the symmetry properties of the considered system. Expression (27) shows that the reflected field consists only of the r mode of the field reemitted by the TLS.

As seen in Eqs. (25) and (27), in order to calculate the photon phase-space distributions we should know two-time correlator $\langle \sigma_+(t)\,\sigma_-(t')\rangle$ and matrix elements $\langle 1_{\alpha,\beta}|\sigma_-(t)|2\rangle$. As follows from (18) evolution of $\langle \sigma_+(t)\,\sigma_-(t')\rangle$ is governed by the equation

$$(\partial_t - i\,\Delta + \Gamma/2)\,\langle \sigma_+(t)\,\sigma_-(t')\rangle$$
$$= i\,g\,\nu[A^*(t)\langle 1_\beta| + B^*(t)\langle 1_\alpha| - 2\,A^*(t)\langle 1_\beta|\sigma_+(t)|0\rangle\langle 0|\sigma_-(t)$$
$$- 2\,B^*(t)\langle 1_\alpha|\sigma_+(t)|0\rangle\langle 0|\sigma_-(t)]\sigma_-(t')|2\rangle. \quad (28)$$

The equation of motion for matrix element $\langle 0|\sigma_-(t)\,\sigma_-(t')|2\rangle$ in the right-hand side of Eq. (28) is given by

$$(\partial_t + i\,\Delta + \Gamma/2)\,\langle 0|\sigma_-(t)\,\sigma_-(t')|2\rangle$$
$$= -i\,g\,\nu[A(t)\,\langle 0|\sigma_-(t')|1_\beta\rangle + B(t)\,\langle 0|\sigma_-(t')|1_\alpha\rangle]. \quad (29)$$

The property $\sigma_-(t)|1_{\alpha,\beta}\rangle = [\langle 1_{\alpha,\beta}|\sigma_+(t)]^\dagger$ and the relation

$$\sigma_-(t)|1_{\alpha,\beta}\rangle = \langle 0|\sigma_-(t)|1_{\alpha,\beta}\rangle|0\rangle,$$
$$\langle 1_{\alpha,\beta}|\sigma_+(t) = \langle 0|\sigma_-(t)|1_{\alpha,\beta}\rangle^*\langle 0| \quad (30)$$

derived in Appendix A are utilized to obtain the right-hand side of Eqs. (28) and (29).

It is assumed that $t > t'$ in Eq. (28). (For $t < t'$ the relation $\langle \sigma_+(t')\,\sigma_-(t)\rangle = \langle \sigma_+(t)\,\sigma_-(t')\rangle^*$ is used.) Thus, for $t = t'$ we get the initial conditions $\langle \sigma_+(t)\,\sigma_-(t')\rangle|_{t=t'} = \langle \sigma_+\,\sigma_-\rangle|_t$ and $\langle 0|\sigma_-(t)\,\sigma_-(t')|2\rangle|_{t=t'} = 0$. Generalization of the described

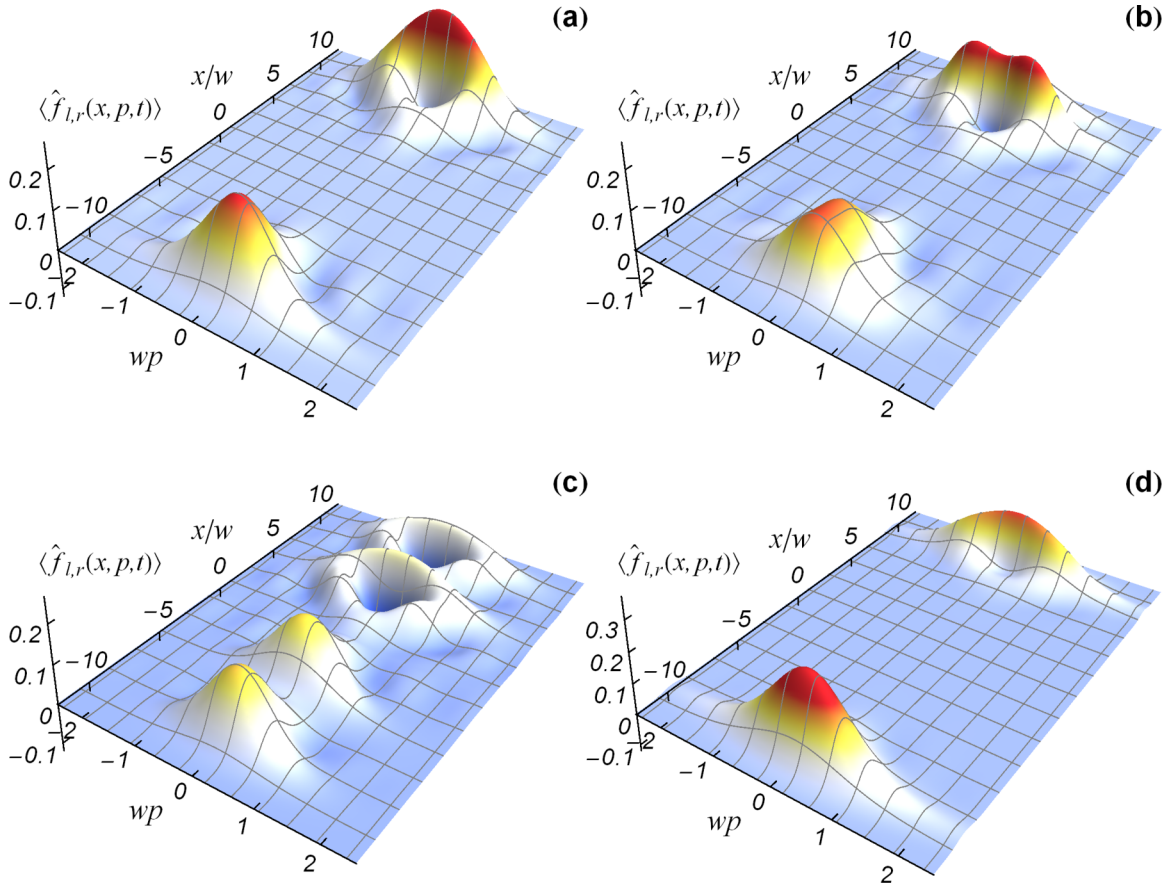

FIG. 5. (Color online) Phase-space distribution for photons after interaction with TLS for different Γ and L. All calculations are performed for $t = (10\,w + |x_0|)/v_g$, $x_0 = -10\,w$ and $\Delta = 0$. The other parameters are the following: (a) $\Gamma = \Omega$, $L = 0$; (b) $\Gamma = \Omega$, $L = 2w$; (c) $\Gamma = \Omega$, $L = 5w$; (d) $\Gamma = 2\Omega$, $L = 0$. Phase-space distributions (a)–(c) exhibit negative values while distribution (d) does not.

scheme for the case of an n-photon Fock state is presented in Appendix B.

Figure 5 shows phase-space distributions of photons after their interaction with the TLS for different values of L and Γ. In contrast to the positive initial distribution (26), the phase-space distribution of transmitted photons ($x > 0$) exhibits a distinct dip, which can form an area of negative values. This is the result of anticorrelation between the ingoing and reemitted fields. When single-photon components of the ingoing state (10) have significant overlap, the dip in the phase-space distribution is less pronounced than in the case of single-photon input considered in Ref. [21]. With increase of Γ the negative regions in the phase-space distribution vanish. The reason for this is that for greater coupling g the qubit is excited more effectively and the term describing the TLS reemission in Eq. (25) dominates the interference term. With increase of the spatial separation L the interference between the initial pulses decays. For large L the problem reduces to the scattering of independent single-photon pulses.

C. Photon densities and spectra

The average photon densities $\langle \hat{\rho}_{l,r}(x,t) \rangle$ can be obtained by integrating the phase-space distribution functions over all momenta $\langle \hat{\rho}_{l,r}(x,t) \rangle = \int dp\, \langle \hat{f}_{l,r}(x,p,t) \rangle$. The results of calculation of $\langle \hat{\rho}_{l,r}(x,t) \rangle$ are shown in Fig. 6.

Increase of the reflection can be seen if the qubit-waveguide coupling Γ or pulse width w increases (see, for example, Refs. [9,16,21]). Stronger waveguide-qubit coupling (or longer ingoing pulses) results in greater probability of the TLS to be excited that leads to more pronounced destructive interference effects in the transmitted field.

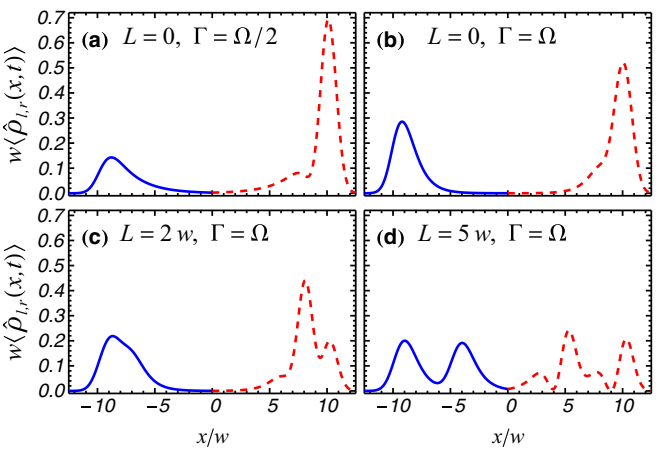

FIG. 6. (Color online) Configuration-space densities of the transmitted (dashed red lines) and reflected (solid blue lines) photons. The rest of the parameters are the same as in Fig. 5.

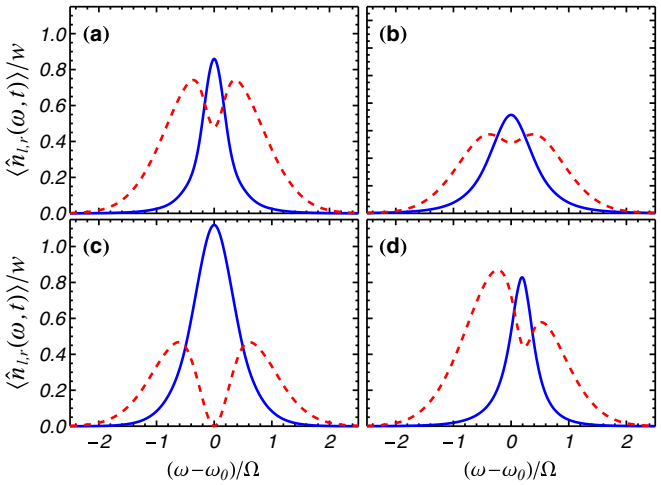

FIG. 7. (Color online) Spectra of the transmitted (red dashed lines) and reflected (blue solid lines) light. Parameters are the following: (a) $\Gamma = \Omega/2$, $L = 0$, $\Delta = 0$; (b) $\Gamma = \Omega$, $L = 0$, $\Delta = 0$; (c) $\Gamma = \Omega$, $L = 10w$, $\Delta = 0$; (d) $\Gamma = \Omega/2$, $L = 0$, $\Delta = \Omega/5$. The calculations are performed for $t \gg \Gamma^{-1} + |x_0|/v_g$ that ensures the outgoing pulses to be far from the TLS; $x_0 = -10\,w$.

Similar reasonings, but expressed in different terms, are applicable for explanation of the features of the outgoing photon spectra. Integration of the phase-space distribution over spatial variable gives the momentum-space distribution. For linear dependencies of $\omega^{l,r}$ on p the relations between the photon momenta and frequency are given by $p = \pm(\omega - \omega_0)/v_g$, where the sign "+" ("−") corresponds to the l mode (r mode), respectively. Thus, the spectra of the outgoing light are determined as

$$\langle \hat{n}_{l,r}(\omega,t)\rangle = \int dx\, \langle \hat{f}_{l,r}(x, \pm(\omega-\omega_0)/v_g, t)\rangle.$$

Figure 7 represents the outgoing light spectra for different parameters of the system.

The TLS emission spectrum has a maximum at ω_a with linewidth Γ. Thus, the maximal TLS excitation and reflection occurs at resonance $\omega_0 = \omega_a$. If the bandwidth of the ingoing wave packet is larger than the linewidth of the TLS emission, only the frequencies close to the resonance $\omega - \omega_0 = \Delta$ provide an effective photon-TLS interaction. The portions of the ingoing wave packet with frequencies far from the resonance pass the TLS almost freely. That is why the spectrum of the reflected light has width Γ and maximum at $\omega - \omega_0 = \Delta$. The transmitted light spectrum has a pronounced minimum at this point. The TLS operates here as a quantum spectral filter resembling a band-stop filter in radioelectronics. For $\Delta = 0$ the spectra of the reflected and transmitted light are symmetric with respect to the point $\omega - \omega_0 = 0$. For $\Delta \neq 0$ the spectra become asymmetric. When the ingoing state consists of two strongly overlapping components, $\langle \hat{n}_l(\omega)\rangle$ does not drop to zero at $\omega - \omega_0 = \Delta$ while for the single-photon input $\langle \hat{n}_l(\omega)\rangle = 0$ at this frequency (see Ref. [21]). This is because only one photon can be absorbed by the TLS at a moment.

IV. PHOTON STATISTICS

Photon number fluctuations of the outgoing light are described by the variances $\langle \delta\hat{N}^2_{l,r}\rangle = \langle(\hat{N}_{l,r} - \langle\hat{N}_{l,r}\rangle)^2\rangle = \langle\hat{N}^2_{l,r}\rangle - \langle\hat{N}_{l,r}\rangle^2$. The further consideration is for $t \gg |x_0|/v_g + \Gamma^{-1}$ when the outgoing pulses are far from the TLS. In this case the average numbers of reflected and transmitted photons do not depend on time. They are connected by the relation

$$\langle\hat{N}_l\rangle = \langle\hat{N}_0\rangle - \langle\hat{N}_r\rangle, \tag{31}$$

where $\hat{N}_0 = \hat{N}_l(t=0)$ is the operator of the number of ingoing photons. Using relation (31) and taking into account $\langle\delta N^2_0\rangle = 0$ for any Fock state we obtain that variances of the reflected and transmitted photon numbers are equal: $\langle\delta\hat{N}^2_l\rangle = \langle\delta\hat{N}^2_r\rangle$. To calculate $\langle\delta\hat{N}^2_r\rangle$ the values of $\langle\hat{N}^2_r\rangle$ and $\langle\hat{N}_r\rangle$ are required. The average number of the reflected photons is defined by

$$\langle\hat{N}_r\rangle = \int dx \int dp\, \langle\hat{f}_r(x,p)\rangle,$$

which with the help of Eq. (27) gives

$$\langle\hat{N}_r\rangle = \frac{\Gamma}{2}\int_0^t d\tau\, \langle\sigma_+\sigma_-\rangle_\tau. \tag{32}$$

The integrand in (32) is governed by Eq. (19a). For $\hat{N}^2_r$ we can use the representation $\hat{N}^2_r = \int dx_1 \int dx_2\, r^\dagger(x_1)\, r^\dagger(x_2)\, r(x_2)\, r(x_1) + \hat{N}_r$. Taking into account Eqs. (22b) and (23b) we obtain

$$\langle\hat{N}^2_r\rangle = \frac{\Gamma^2}{2}\int_0^t d\tau \int_0^\tau d\tau'\, \langle\sigma_+(\tau')\,\sigma_+(\tau)\,\sigma_-(\tau)\,\sigma_-(\tau')\rangle + \langle\hat{N}_r\rangle.$$

Using the property

$$\sigma_-(t)\,\sigma_-(t')|2\rangle = \langle 0|\sigma_-(t)\,\sigma_-(t')|2\rangle|0\rangle, \tag{33}$$

derived in Appendix A, we get

$$\langle\hat{N}^2_r\rangle = \frac{\Gamma^2}{2}\int_0^t d\tau \int_0^\tau d\tau'\, |\langle 0|\sigma_-(\tau)\,\sigma_-(\tau')|2\rangle|^2 + \langle\hat{N}_r\rangle. \tag{34}$$

The matrix element $\langle 0|\sigma_-(t)\,\sigma_-(t')|2\rangle$ in (34) obeys Eq. (29).

The results of calculations shown in Fig. 8 confirm the tendency of reflectance to increase when the waveguide-TLS coupling increases. This tendency becomes more pronounced for greater L. Also we can see that the variance of the reflected photons is less than the average photon number for any Γ and L. This manifests the sub-Poissonian statistics of the reflected photons, which are emitted one by one by the TLS. In contrast, the transmitted light can exhibit super-Poissonian statistics.

V. SUMMARY

Our approach provides a detailed picture of the interaction of two-photon pulses with TLS. This makes it possible to describe not only the asymptotic characteristics of the outgoing light, such as transmission and reflection coefficients or photon scattering probabilities [14–16], but also to investigate the dynamics of the whole system (see Fig. 5). A full set of equations describing the evolution of the two-photon state is derived and solved for different parameters. It is shown that

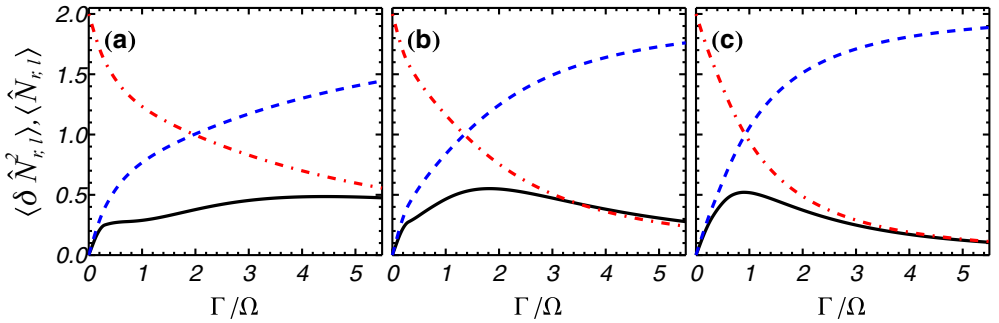

FIG. 8. (Color online) Variances of outgoing photon numbers (solid black lines) and the average numbers of reflected (dashed blue lines) and transmitted (dash-dotted red lines) photons vs Γ at $\Delta = 0$ for different (a) L: $L = 0$, (b) $L = 2w$, and (c) $L = 5w$.

along with the coupling strength g and the initial pulse width the spatial separation between the single-photon components of the ingoing field strongly affects the dynamics of the system.

The method of photon phase-space operator has an advantage of high universality. Its integration over the momentum p results in the photon density in the configuration space (see Fig. 6). Similarly, integration of the phase-space distribution over the configuration space gives light spectra. Our calculations show that spectra of the reflected and transmitted photons have distinct differences due to peculiarities of the TLS response. Owing to the saturable behavior of the TLS excitation the spectra of the outgoing light for the two-photon input differ from those for the single-photon input (see Ref. [21]).

We have studied photon number fluctuations of the outgoing light. The corresponding variances for both modes are found to be equal for any n-photon Fock state. These variances determine signal-to-noise ratios that describe the possibility of outgoing light to be utilized. Dependence of the variances on the coupling parameter g and the separation distance L is analyzed. Our calculations show the presence of only sub-Poissonian statistics of the reflected photons regardless of the choice of Γ and L. By contrast, the statistics of the transmitted photons can be sub-Poissonian or super-Poissonian depending on choice of the parameters Γ and L.

To summarize, tuning both the waveguide-TLS coupling and the ingoing pulse separation can control both the state of the qubit and statistical characteristics of the outgoing light. This may find applications in quantum information processing.

ACKNOWLEDGMENTS

The authors thank V. Bondarenko, S. Lukyanets, and A. Semenov for useful discussions and comments.

APPENDIX A: OPERATOR PROPERTIES

1. Properties of free-moving operators

Here we prove the commutation relations

$$\left[\int dp\, \tilde{l}_p(t), \sigma_-(t')\right] = \left[\int dp\, \tilde{r}_p(t), \sigma_-(t')\right] = 0, \quad t \geqslant t'. \tag{A1}$$

Using the representation $\tilde{l}_p(t) = \tilde{l}_p(t')\, e^{-i\, v_g\, p\, (t-t')}$, equal-time commutator $[l_p, \sigma_-] = 0$ and Eq. (15a) we obtain

$$\left[\int dp\, \tilde{l}_p(t), \sigma_-(t')\right] = \int dp\, e^{-i\, v_g\, p\, (t-t')} \left[l_p(t') + i\, g \int_0^{t'} d\tau\, e^{-i\, v_g\, p\, (t'-\tau)}\, \sigma_-(\tau), \sigma_-(t') \right]$$

$$= i\, g \int dp \int_0^{t'} d\tau\, e^{-i\, v_g\, p\, (t-\tau)} [\sigma_-(\tau), \sigma_-(t')] = i\, \frac{2\pi\, g}{v_g} [\sigma_-(t), \sigma_-(t')] \theta(t' - t).$$

Presence of the θ function in the last term shows that the initial expression is equal to zero if $t > t'$. When $t = t'$ the commutator $[\sigma_-(t), \sigma_-(t')]$ is equal to zero. This proves Eq. (A1). Similar reasonings are applicable for the second commutator in (A1).

It follows directly from the definitions of the free-moving operators (15), the single-photon states (6), and the two-photon states (10) that

$$\int dp\, \tilde{l}_p(t) |1_\alpha\rangle = A(t)|0\rangle, \quad \int dp\, \tilde{l}_p(t) |1_\beta\rangle = B(t)|0\rangle, \tag{A2}$$

$$\int dp\, \tilde{l}_p(t) |2\rangle = v[A(t)|1_\beta\rangle + B(t)|1_\alpha\rangle] \tag{A3}$$

and

$$\tilde{r}_p(t)|2\rangle = \tilde{r}_p(t)|1_\alpha\rangle = \tilde{r}_p(t)|1_\beta\rangle = 0. \tag{A4}$$

These relations are widely used in the paper.

2. Derivation of the relations (30) and (33)

The action of $\sigma_-(t)$ on the states $|1_{\alpha,\beta}\rangle$ gives the state $C_{\alpha,\beta}(t)|0\rangle$. To prove this we use the solution of Eq. (18):

$$\sigma_-(t) = \tilde{\sigma}_-(t) + i\, g \int_{t_0}^{t} d\tau\, e^{-(i\,\Delta + \Gamma/2)(t-\tau)} \times (2\,\sigma_+\,\sigma_-|_\tau - 1) \int dp\, (\tilde{l}_p + \tilde{r}_p)|_\tau. \tag{A5}$$

With account for the relation $\sigma_-(t)|0\rangle = \tilde{\sigma}_-(t)|1_{\alpha,\beta}\rangle = 0$ and Eq. (A5), we have

$$\sigma_-(t)|1_\alpha\rangle = -i\,g\int_{t_0}^{t} d\tau\, e^{-(i\,\Delta+\Gamma/2)(t-\tau)}\,A(\tau)|0\rangle. \quad \text{(A6)}$$

The expression for the state $|1_\beta\rangle$ can be obtained from (A6) by replacing $A(t)$ with $B(t)$.

As we see, the action of the lowering operator $\sigma_-(t)$ on the single-photon state $|1_{\alpha,\beta}\rangle$ moves the system into the vacuum state $|0\rangle$

$$\sigma_-(t)|1_{\alpha,\beta}\rangle = C_{\alpha,\beta}(t)|0\rangle, \quad \text{(A7)}$$

where the factor $C_{\alpha,\beta}(t)$ is given by (A6). It follows from Eq. (A7) that the state $\sigma_-(t)|1_{\alpha,\beta}\rangle$ can be represented in the equivalent form

$$\sigma_-(t)|1_{\alpha,\beta}\rangle = \langle 0|\sigma_-(t)|1_{\alpha,\beta}\rangle|0\rangle, \quad \text{(A8)}$$

where $\langle 0|\sigma_-(t)|1_{\alpha,\beta}\rangle \equiv C_{\alpha,\beta}(t)$.

Similarly we can prove that $\sigma_-(t)\,\sigma_-(t')|2\rangle = \langle 0|\sigma_-(t)\,\sigma_-(t')|2\rangle|0\rangle$. Taking into account (A1), (A3), and (A4) the equation of motion for $\sigma_-(t)\,\sigma_-(t')|2\rangle$ for $t > t'$ has the form

$$\begin{aligned}&(\partial_t + i\,\Delta + \Gamma/2)\,\sigma_-(t)\,\sigma_-(t')|2\rangle\\ &\quad = i\,g\,\nu\,(2\,\sigma_+\,\sigma_-|_t - 1)\,\sigma_-(t')[A(t)|1_\beta\rangle + B(t)|1_\alpha\rangle], \quad \text{(A9)}\end{aligned}$$

with solution

$$\begin{aligned}&\sigma_-(t)\,\sigma_-(t')|2\rangle\\ &\quad = i\,g\,\nu\int_{t'}^{t} d\tau\, e^{-(i\,\Delta+\Gamma/2)(t-\tau)}\,(2\,\sigma_+\,\sigma_-|_\tau - 1)\;\sigma_-(t')\\ &\qquad \times [A(\tau)|1_\beta\rangle + B(\tau)|1_\alpha\rangle].\end{aligned}$$

Due to relation (A8) and property $\sigma_+\,\sigma_-|0\rangle = 0$ we obtain

$$\begin{aligned}\sigma_-(t)\,\sigma_-(t')|2\rangle = -i\,g\,\nu\int_{t'}^{t} d\tau\, e^{-(i\,\Delta+\Gamma/2)(t-\tau)}\\ \times [A(\tau)\,C_\beta(t') + B(\tau)\,C_\alpha(t')]|0\rangle. \quad \text{(A10)}\end{aligned}$$

Thus, the state $\sigma_-(t)\,\sigma_-(t')|2\rangle$ can be represented as

$$\sigma_-(t)\,\sigma_-(t')|2\rangle = \langle 0|\sigma_-(t)\,\sigma_-(t')|2\rangle|0\rangle. \quad \text{(A11)}$$

APPENDIX B: *n*-PHOTON FOCK STATE

The previous considerations can be extended for the n-photon Fock state defined as

$$\left|n_{\{\alpha_j\}}\right\rangle = \nu_n \prod_{j=1,n} a^\dagger_{\alpha_j}|0\rangle, \quad \text{(B1)}$$

where ν_n is the normalization constant. Fock states form a subset of more general n-photon states [27] whose interaction with an arbitrary quantum system is investigates in Ref. [28]. We restrict ourselves with the n-photon Fock states given by (B1). For simplicity, we consider $\alpha_j = \alpha$ and (B1) reduces to

$$|n_\alpha\rangle = \frac{1}{\sqrt{n!}}[a^\dagger_\alpha]^n|0\rangle. \quad \text{(B2)}$$

For the state (B2) the initial configuration-space density of photons is given by the single-peak distribution

$$\langle n|\hat{\rho}(x,t=0)|n\rangle = \frac{n}{\sqrt{\pi}\,w}\,e^{-(x-x_0)^2/w^2}$$

that coincides with the density in the two-photon state (10) when $n = 2$, $L = 0$, and $|1_\alpha\rangle = |1_\beta\rangle$.

Let us consider calculation of the average number of reflected and transmitted photons. When $t \to \infty$, the average numbers of reflected and transmitted photons are coupled by the condition $\langle\hat{N}_l\rangle = n - \langle\hat{N}_r\rangle$, where the average number of reflected photons is given by

$$\langle\hat{N}_r\rangle = \frac{\Gamma}{2}\int_0^\infty d\tau\,\langle n|\sigma_+\,\sigma_-|n\rangle_\tau. \quad \text{(B3)}$$

The integrand in (B3) is governed by the equation

$$(\partial_t + \Gamma)\,\langle n|\sigma_+\,\sigma_-|n\rangle = i\,g\,\sqrt{n}\,A^*(t)\,\langle n-1|\sigma_-|n\rangle + \text{c.c.}, \quad \text{(B4)}$$

which follows from Eq. (17). In turn, the matrix element $\langle n-1|\sigma_-|n\rangle$ obeys

$$\begin{aligned}&(\partial_t + i\,\Delta + \Gamma/2)\,\langle n-1|\sigma_-|n\rangle\\ &\quad = 2\,i\,g\,\sqrt{n}\,A(t)\,\langle n-1|\sigma_+\,\sigma_-|n-1\rangle - i\,g\,\sqrt{n}\,A(t). \quad \text{(B5)}\end{aligned}$$

To obtain Eqs. (B4) and (B5) we have used the relation

$$\int dp[\tilde{l}_p(t) + \tilde{r}_p(t)]|n\rangle = \sqrt{n}\,A(t)\,|n-1\rangle. \quad \text{(B6)}$$

It can be seen that $\langle n|\sigma_+\,\sigma_-|n\rangle$ depends on $\langle n-1|\sigma_-|n\rangle$, which in turn depends on $\langle n-1|\sigma_+\,\sigma_-|n-1\rangle$ and so on down to $\langle 1|\sigma_+\,\sigma_-|1\rangle$ and $\langle 0|\sigma_-|1\rangle$. This set of $2n$ coupled equations should be complemented by the initial conditions $\langle m|\sigma_+\,\sigma_-|m\rangle|_{t=0} = \langle m-1|\sigma_-|m\rangle|_{t=0} = 0$, where $1 \leqslant m \leqslant n$. For $n = 1$ we can use (30) and write $\langle 1|\sigma_+\,\sigma_-|1\rangle = \langle 1|\sigma_+|0\rangle\langle 0|\sigma_-|1\rangle = |\langle 0|\sigma_-|1\rangle|^2$, where $\langle 0|\sigma_-|1\rangle$ is given by (20).

The two-time correlation function $\langle n|\sigma_+(t)\,\sigma_-(t')|n\rangle$ is required for calculation of the phase-space distributions [see Eqs. (25) and (27)]. The equation of motion for $\langle n|\sigma_+(t)\,\sigma_-(t')|n\rangle$ is given by

$$\begin{aligned}&(\partial_t - i\,\Delta + \Gamma/2)\,\langle n|\sigma_+(t)\,\sigma_-(t')|n\rangle\\ &\quad = -2\,i\,g\,\sqrt{n}\,A^*(t)\,\langle n-1|\sigma_+(t)\,\sigma_-(t)\,\sigma_-(t')|n\rangle\\ &\qquad + i\,g\,\sqrt{n}\,A^*(t)\,\langle n-1|\sigma_-(t')|n\rangle, \quad \text{(B7)}\end{aligned}$$

where the initial value $\langle n|\sigma_+(t=t')\,\sigma_-(t')|n\rangle$ is taken from solution of Eqs. (B4) and (B5). The evolution of $\langle n-1|\sigma_+(t)\,\sigma_-(t)\,\sigma_-(t')|n\rangle$ is governed by

$$\begin{aligned}&(\partial_t + \Gamma)\,\langle n-1|\sigma_+(t)\,\sigma_-(t)\,\sigma_-(t')|n\rangle\\ &\quad = i\,g\,\sqrt{n-1}\,A^*(t)\,\langle n-2|\sigma_-(t)\,\sigma_-(t')|n\rangle\\ &\qquad - i\,g\,\sqrt{n}\,A(t)\,\langle n-1|\sigma_+(t)\,\sigma_-(t')|n-1\rangle. \quad \text{(B8)}\end{aligned}$$

The equation of motion for $\langle n-1|\sigma_+(t)\,\sigma_-(t')|n-1\rangle$ entering the right-hand side of (B8) is

$$\begin{aligned}(\partial_t + i\,\Delta + \Gamma/2)\,\langle n-2|\sigma_-(t)\,\sigma_-(t')|n\rangle \\ = 2\,i\,g\,\sqrt{n}\,A(t)\,\langle n-2|\sigma_+(t)\,\sigma_-(t)\,\sigma_-(t')|n-1\rangle \\ -i\,g\,\sqrt{n}\,A(t)\,\langle n-2|\sigma_-(t')|n-1\rangle. \qquad \text{(B9)}\end{aligned}$$

We have used (A1) to derive Eqs. (B7), (B8), and (B9). Zero-value initial conditions (at $t = t'$) should be imposed for solutions of Eqs. (B8) and (B9). Equations (B7)–(B9) show that $\langle n|\sigma_+(t)\,\sigma_-(t')|n\rangle$ can be expressed via two-time functions with lower values of n (down to $n = 1$). For $\langle 1|\sigma_+(t)\,\sigma_-(t')|1\rangle$ we can use the explicit expression obtained with the use of (30) and (20):

$$\begin{aligned}\langle 1|\sigma_+(t)\,\sigma_-(t')|1\rangle = g^2 \int_0^t d\tau\, e^{(i\,\Delta-\Gamma/2)(t-\tau)}\,A^*(\tau) \\ \times \int_0^{t'} d\tau\, e^{-(i\,\Delta+\Gamma/2)(t'-\tau)}\,A(\tau). \qquad \text{(B10)}\end{aligned}$$

The two-time correlators $\langle\sigma(t')\,\sigma(t)\rangle$ are also useful for calculation of the cross correlations between the TLS and the reemitted field. The first-order cross-correlation function can be defined as $X_r^{(1)}(\tau) = \langle\hat{E}_r^{(-)}(x,t)\,\sigma_-(t+\tau)\rangle$, where the negative frequency part of the field is expressed in terms of photonic operators as $\hat{E}_r^{(-)}(x,t) \propto r^\dagger(x,t)$. Using Eqs. (22) we obtain $X_r^{(1)}(\tau) \propto \langle\sigma_+(t + x/v_g)\,\sigma_-(t+\tau)\rangle$, where the equation of motion for the right-hand side is given by (B7).

[1] J. I. Cirac and P. Zoller, Phys. Rev. Lett. **74**, 4091 (1995).
[2] C. Monroe, D. Leibfried, B. E. King, D. M. Meekhof, W. M. Itano, and D. J. Wineland, Phys. Rev. A **55**, R2489 (1997).
[3] I. H. Deutsch and P. S. Jessen, Phys. Rev. A **57**, 1972 (1998).
[4] A. Wallraff, D. I. Schuster, A. Blais, L. Frunzio, J. Majer, M. H. Devoret, S. M. Girvin, and R. J. Schoelkopf, Phys. Rev. Lett. **95**, 060501 (2005).
[5] F. Henneberger and O. Benson, *Semiconductor Quantum Bits* (Pan Stanford, Singapore, 2008).
[6] D. N. Matsukevich, T. Chaneliere, S. D. Jenkins, S.-Y. Lan, T. A. B. Kennedy, and A. Kuzmich, Phys. Rev. Lett. **96**, 030405 (2006)
[7] D. L. Moehring, P. Maunz, S. Olmschenk, K. C. Younge, D. N. Matsukevich, L.-M. Duan, and C. Monroe, Nature Lett. **449** 68 (2007).
[8] A. Blais, R. S. Huang, A. Wallraff, S. M. Girvin, and R. J. Schoelkopf, Phys. Rev. A **69**, 062320 (2004).
[9] P. Domokos, P. Horak, and H. Ritsch, Phys. Rev. A **65**, 033832 (2002).
[10] K. Kojima, H. F. Hofmann, S. Takeuchi, and K. Sasaki, Phys. Rev. A **68**, 013803 (2003).
[11] H. F. Hofmann, K. Kojima, S. Takeuchi, and K. Sasaki, Phys. Rev. A **68**, 043813 (2003).
[12] V. I. Yudson and P. Reineker, Phys. Rev. A **78**, 052713 (2008).
[13] J.-T. Shen and S. Fan, Phys. Rev. Lett. **98**, 153003 (2007).
[14] J.-T. Shen and S. Fan, Phys. Rev. A **76**, 062709 (2007).
[15] S. Xu, E. Rephaeli, and S. Fan, Phys. Rev. Lett. **111**, 223602 (2013).
[16] H. Zheng, D. J. Gauthier, and H. U. Baranger, Phys. Rev. A **82**, 063816 (2010).
[17] S. Fan, S. E. Kocabaş, and J.-T. Shen, Phys. Rev. A **82**, 063821 (2010).
[18] E. Rephaeli, S. E. Kocabaş, and S. Fan, Phys. Rev. A **84**, 063832 (2011).
[19] W. Vogel and D.-G. Welsch, *Quantum Optics* (Wiley-VCH, Weinheim, 2006); C. W. Gardiner and P. Zoller, *Quantum Noise* (Springer, Berlin, 2010).
[20] G. P. Berman and A. A. Chumak, Phys. Rev. A **74**, 013805 (2006); G. P. Berman, A. A. Chumak, and V. N. Gorshkov, Phys. Rev. E **76**, 056606 (2007); G. P. Berman and A. A. Chumak, Proc. of SPIE **6710**, 67100M (2007).
[21] O. O. Chumak and E. V. Stolyarov, Phys. Rev. A **88**, 013855 (2013).
[22] J. T. Shen and S. Fan, Opt. Lett. **30**, 2001 (2005).
[23] J. T. Shen and S. Fan, Phys. Rev. A **79**, 023837 (2009).
[24] K. J. Blow, R. Loudon, S. J. D. Phoenix, and T. J. Shepherd, Phys. Rev. A **42**, 4102 (1990).
[25] H. Oka, Phys. Rev. A **81**, 053837 (2010); Opt. Express **18**, 25839 (2010).
[26] A. A. Tarasenko and A. A. Chumak, Sov. Phys. JETP **46**, 327 (1977).
[27] P. Rohde, W. Mauerer, and C. Silberhorn, New J. Phys. **9**, 91 (2007).
[28] B. Q. Baragiola, R. L. Cook, A. M. Brańczyk, and J. Combes, Phys. Rev. A **86**, 013811 (2012).